PCCP

Accepted Manuscript

ROYAL SOCIETY OF CHEMISTRY

www.rsc.org/pccp

Calorimetric and Spectroscopic Studies on the Solvation Energetics for H_2 Storage in the CO_2/HCOOH System

Cornel Fink, Sergey Katsyuba, Gabor Laurenczy*

Abstract:

Solvents play a crucial role in many chemical reactions and additives can be used to shift the reaction equilibrium. Herein we study the enthalpy of mixing for selected solvents (aqueous, organic) and basic additives (amines, aqueous KOH) when mixed with formic acid with the aim to optimize hydrogen storage/delivery in the CO_2/HCOOH system. Formic acid, resulting from carbon dioxide hydrogenation, reaches highest yields when effectively "removed" from the reaction equilibrium. In terms of energy efficiency, any heat release during CO_2 hydrogenation has to be reinvested in the reverse reaction, during the production of hydrogen. In any scenario, the usage of basic chemicals, non innocent solvents causes higher energy release in the CO_2 hydrogenation, which as to be reinvested in the hydrogen delivery process. Therefore, the enthalpy of mixing is a valuable parameter for designing hydrogen storage devices since it allows to estimate the energy balance for the CO_2 hydrogenation/H_2 liberation cycle.

The highest formic acid concentrations in direct catalytic CO_2 hydrogenation under acidic conditions were reached in DMSO. DMSO exhibits considerably stronger interactions with formic acid compared to water as was observed in calorimetric measurements. This difference can be ascribed, at least partly, to stronger hydrogen bonding of FA to DMSO than to water in the corresponding solutions, examined by a combination of IR spectroscopic and quantum chemical studies. Furthermore, the investigation of the DMSO/FA- and water/FA systems by ^{1}H- and ^{13}C-NMR spectroscopy revealed that only 1:1 aggregates are formed in the DMSO solutions of FA in a broad concentration range, while the stoichiometry and the number of the FA-water aggregates essentially depends on the concentration of the aqueous solutions.

Keywords: *formic acid, carbon dioxide utilization, , enthalpy of mixing for binary formic acid mixtures; adduct formation, basic additives, formic acid dehydrogenation, carbon dioxide hydrogenation, hydrogen storage, calorimetry*

Introduction

Fossils fuels account for the majority of our energy needs, such as heat, electricity, and transportation.[1-3] The exploitation of these energy reserves by simple combustion processes releases vast amounts of gases into the atmosphere, mainly CO_2 (35.3 Gt/a)[4], SO_2 and NO_2. The consequences are well known as the greenhouse effect and acid rain.[5] Since it seems unlikely that the dependency on fossil energy sources will change considerably in the near future, a possible solution to decrease the anthropogenic CO_2 emission is to capture the emerging CO_2 at its origin[6] and recycle it by e.g. reducing it with hydrogen ($\Delta G°_{CO2(g)}$ = +33 kJ/mol), produced with energy from renewable energy sources. Carbon dioxide utilized as C_1 building block[7] allows the production of a series of feedstock chemicals, but only a small fraction (about 0.5-1%) of anthropogenic carbon dioxide is presently used in global chemical industry for urea (110 Mt/a), salicylic acid (30 Mt/a), or methanol (2 Mt/a).[8, 9] Nature in contrast uses CO_2 as carbon source to build up the whole biosphere.[10] Formic acid (FA) has a comparable high hydrogen content (53 g/L), which makes it attractive as an easy accessible secondary energy vector for a future hydrogen-based society.[11-15] Generally, the formic acid/carbon dioxide cycle for hydrogen storage (Figure 1) can be divided into two parts, namely the FA production (CO_2 hydrogenation) and FA consumption (hydrogen delivery). The gas phase reaction of FA formation exhibits a positive ΔG° value (entropic contribution, $\Delta G°_{(g)}$ = +33 kJ/mol), the reaction is already more favored in water ($\Delta G°_{CO2(water)}$ = -4 kJ/mol),[16] and under basic conditions (additives or basic solvents), the reaction equilibrium is shifted to the product side ($\Delta G°_{bicarbonate}$ = -35 kJ/mol).[17-20] Calorimetric measurements in this paper quantify the heat which is liberated when formic acid solvates in the reaction solvent, a parameter that becomes relevant for the energy balance when performing the reverse reaction, the delivery of hydrogen from formic acid in its respective liquid matrix.

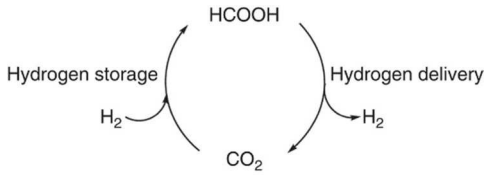

Figure 1 Formic acid/carbon dioxide cycle for hydrogen storage and delivery

Reagent + status	ΔG° (kJ mol^{-1})	products + status
$CO_{2(g)} + H_{2(g)}$	32.9	$HCO_2H_{(l)}$
$CO_{2(aq)} + H_{2(aq)}$	-4	$HCO_2H_{(aq)}$
$CO_{2(aq)} + H_{2(aq)} + NH_{3(aq)}$	-9.5	$HCO_2^-{}_{(aq)}\ NH_4^+{}_{(aq)}$
$CO_{2(aq)} + H_{2(aq)} + Base_{(aq)}$	-35	$HCO_2^-{}_{(aq)} + BaseH^+{}_{(aq)}$
$MHCO_{3(aq)} + H_{2(aq)}$	-0.72	$MHCO_{2(aq)} + H_2O_{(l)}$

Table 1 Thermodynamic data for the conversion of CO_2 and H_2 into HCO_2H under various conditions[19, 21]

An important factor for maintaining the efficiency of a chemical reaction is the stabilization or removal of products from the equilibrium mixture. This can be achieved on different ways, probably the most favorable would be an "online" physical separation of products. In case of CO_2 hydrogenation, the topic is under current research but a widely accepted solution was not presented yet.[22, 23] Another approach is "to remove" the formic acid chemically from the equilibrium mixture by continuously reacting it with either an additive, solvent or a combination of both, in a nutshell, to stabilize it.[17] As mentioned previously, basic conditions allow to reach high formate concentrations in comparably short reaction times. The field of carbon dioxide as raw material for the FA synthesis was reviewed by Leitner in 2003[20], Jessop *et al.* in 2004,[24] and Federsel *et al.*, 2010.[25] More recently, in 2013, Sanford *et al.*

reported on catalytic CO_2 hydrogenation under basic conditions (NEt_3) to formate by a ruthenium pincer complex.[26] A drawback with this procedure is the more laborious purification of produced FA due to the strong intermolecular interactions of formed acid-base adducts[27] and the lower exploitable hydrogen content per weight unit when used directly (2.3 wt% H_2 for typical 5(HCOOH):2(NEt_3) mixtures). Recently, Laurenczy *et al.* informed about reaching unprecedentedly high concentrations of FA (2 M) under acidic conditions with a Ru based catalyst in pure dimethyl sulfoxide (DMSO) without any additives. The same catalyst afforded under similar conditions a 0.2 molar FA solution in acidic aqueous solution.[28]

Beller *et al.* developed several iron[29, 30] and ruthenium[31] catalysts for formic acid dehydrogenation using formic acid-amine mixtures. Advances in the additive and base-free formic acid decomposition have been reported by Laurenczy *et al.*, using a Ru-biaryl sulfonated phosphine species in aqueous solution,[32] Reek *et al.* with a catalytic active Ir–bisMETAMORPhos complex,[33] or Himeda *et al.* with Ir and Rh complexes, coordinating imidazole and pyrazole derived ligands.[34]

Solvents undoubtedly play a central role in a large number of chemical reactions,[35] and they can be categorized by e.g. their role in chemical reactions.[36] Some solvents dissolve the reactants but do not participate in the chemical reaction, while others also have an active role in reaction e.g. serve as source of acids or bases. A typically participating solvent is water. The exothermic interaction between water and FA can be partly explained due to the exoergic protonation of water by the acid.

Some experimental and theoretical studies have been reported on formic acid hydrates. Microwave spectroscopic studies of FA clusters in gas-phase with one or two associated water molecules provided structural information about these species.[37] Results of infrared (IR) measurements of 1(FA):1(water) and 1(FA):2(water) clusters in isolated noble gas matrices are published recently.[38, 39] IR[40, 41] and Raman[42, 43] spectroscopic studies of aqueous solutions of FA are also known. According to the IR analysis, the monomeric neutral form (non-dissociated) of FA is prevalent in 4 mol/dm^3 solutions,[40] however the formation of trace amounts of contact ion pairs at lower concentrations due to FA-water proton transfer cannot be excluded.[41] Raman spectra[42] delivered evidence of the existence of self-associated species of FA in aqueous solutions, ranging from pure FA until dilutions of the acid *X*(HCOOH) = 0.51 (mole fraction). The self-association results in a pronounced splitting of νC=O band of FA. Studies of more diluted mixtures were not performed because of overlaps with the ν_2 Raman band of water. Static structures of "gas-phase" aggregates of FA with up to eight water molecules were calculated and optimized by various quantum-chemical methods.[37, 39, 41, 44-50] The behavior of liquid water/FA systems was studied computationally with molecular dynamics,[47, 51] *ab initio* molecular dynamics,[52] and Monte Carlo simulations.[53]

We also observed notable heat evolution when mixing DMSO and formic acid in calorimetric measurements. Published information about FA interactions with DMSO is very limited. One of the few findings was devoted to quantum-chemical computations of structure and NMR chemical shifts of "gas-phase" 1(FA):1(DMSO) and 1(FA):2(DMSO) aggregates.[50]

Results and Discussion

Calorimetric and Conductometric examination of the water/FA and the DMSO/FA system

Heat flow calorimetry provides quantitative information about endo- and exothermic processes in the reactor chamber.[54] The calorimetric measurements were performed with a Mettler Toledo EasyMax

102 Advanced Synthesis Workstation, equipped with HFCal option for heat flow calorimetry. Typically, one compound was prefilled in the reactor and formic acid was added in small discrete steps.

Formic acid is a medium strong organic acid with a dissociation constant of $K_a = 1.77 \cdot 10^{-4}$ in water[55] and its interaction with water is moderately exothermic compared to strong acids, which in contrast dissociate completely. Starting from pure water (45 g, 2.5 mol), we added FA stepwise (9.234 mL, 0.25 mol, 4x). The total addition of one mole FA (37.72 mL) resulted in steadily increasing mixing enthalpies (Figure 2, addition 1 to 4), a unique reaction behavior, which was different than with any other tested solvent. The molar heat of mixing was found to be 0.76 ± 0.16 kJ (n_{obs} = 3). When the mole fraction of water fell below 0.71, the heat release per addition started to decline as well (Figure 2, addition 5 to 17). In order to obtain data at wide X ratios, we designed experimental series, where FA was added until reaching X(water) = 0.32. The reason to stop at this point was that the last three additions showed negative mixing enthalpies (Figure 2, Add 19 to 21). Under these circumstances, negative mixing enthalpies are an indication for reaching the limit of favorable mixing ratios for the observed system. For all other systems, we found the highest enthalpies when combining the pure chemicals, only for the water/FA system, the curve peaks around a molar ratio X(water) = 0.70 (Figure 2, addition 4 and 5).

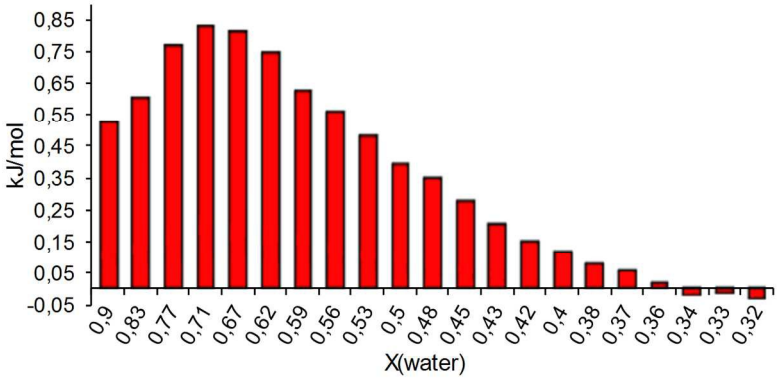

Figure 2 Enthalpies of mixing for water with FA; each column equals an addition of 0.25 mol FA; detailed information about the experimental procedure are given in the "Material and Methods" section

DMSO possesses two potentially basic centers in its S=O group. Accordingly, a protonation could occur at both sites with valence electron pairs on the oxygen **1** or sulfur **2** atom (Figure 3).

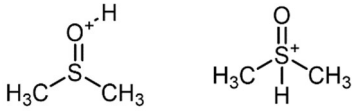

Figure 3 Possible protonation sites on DMSO

Early NMR measurements were not conclusive for either structure,[56-59] but a combination of IR- and Raman spectroscopy[60] and also more recent NMR studies[61] proved structure **1** true, showed that it is 37.0 kcal/mol more stable than structure **2** (Figure 3).[62] In these experiments, super acids were used to fully protonate DMSO e.g. FSO_3H-SbF_5 ("Magic Acid").

The experimental procedure for mixing DMSO with formic acid was an analog to the water/FA approach. DMSO (1.0 mol) was poured into the measuring chamber and FA was added gradually in

discrete steps, each 0.25 mol (9.234 mL). The finding of decreasing heat release at higher dilutions of DMSO with formic acid lived up to the general expectation of registering the highest heat release for combining pure compounds (Figure 4). The molar heat release for this system is 11.6 ± 0.27 kJ/mol (n_{obs} = 3), much higher than any other non-basic solvent.

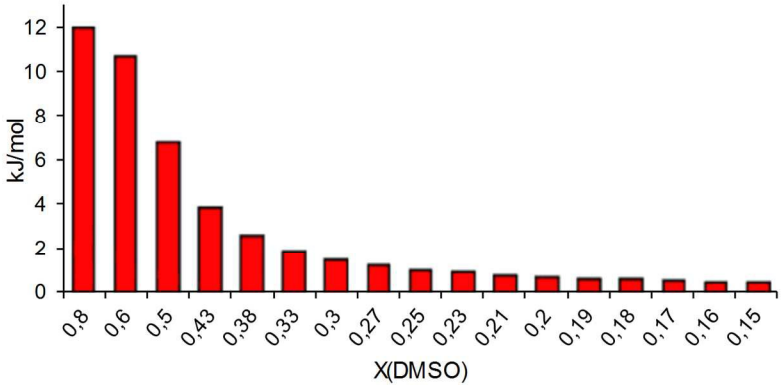

Figure 4 Enthalpies of mixing for DMSO with FA; each addition is equal to or corresponds to 0.25 mol FA (see "Materials and Methods)

Control experiments were also performed to verify if the mode of addition – small steps or bigger volumes - has an influence on the obtained energies. In one experimental series, one mole of FA was added at once to DMSO and the recorded energy release was with 11.3 kJ/mol in the same range as observed during stepwise addition (Table 2, #2). In fact, the reaction of FA and DMSO is significantly more exothermic than for the corresponding water/FA system. On one hand, this remarkable difference was unexpected since DMSO, as a non-protogenic solvent, cannot undergo the highly exothermic formation of solvated hydronium ions.[63] On the other hand, the observed stronger heat development can partly be explained by a higher proton affinity of DMSO[64] compared to water.[65]

The measurement of electrical conductivity (S/m) is a simple and sensitive method to detect nonspecific ionic species in solution.[66] Plausible sources for the heat evolution in the FA/DMSO system are the protonation of DMSO and liberated solvation energy. An increase in conductivity while mixing FA and DMSO would be a strong indication for the formation of charged DMSO-H^+ species and disassociated $HCOO^-$ ions. We designed three different experiments, which were each reproduced in triplicate, to study the processes, namely water/FA, DMSO/methansulfonic acid (MSA, pK_a = -1.9),[67] and DMSO/FA. The addition of 13.2 mmol FA (0.5 mL) to 54 mL deionized water increased its conductivity from 2.38 µS/cm to 2.20 mS/cm (X(water) = 0.99560). The maximal conductivity was 10.2 mS/cm at X(water) = 0.85 and the conductivity decreased at higher formic acid concentrations. The conductivity of dry DMSO was found to be 0.175 ± 0.01 µS/cm and increased when adding anhydrous formic acid to a maximum conductivity of 1.70 mS/cm at X(DMSO) = 0.11 (Figure 5). The increase in conductivity in comparison to pure FA (128 ± 5 µS/cm) is apparent, but the peak value is still six times lower than for the corresponding water/FA system. For the third system, we combined MSA with DMSO

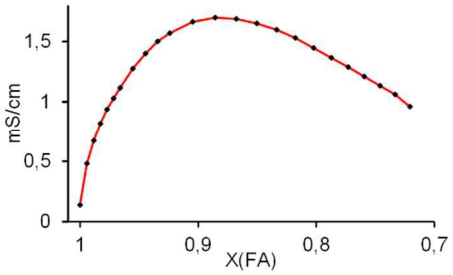

Figure 5 Dependency of the conductivity in the DMSO/FA system on X(formic acid)

and reached an intermediate conductivity of 6.89 mS/cm at X(DMSO) = 0.83. Accordingly, the main source for the heat liberation in the DMSO/FA is not found in an acid-base reaction.

Another factor we considered was the contribution of hydrogen bond formation -and breaking. A series of well-known simple experiments illustrates its role and effect upon the heat of mixing.[68] These experiments, here briefly summarized, started by mixing two hydrogen bonded liquids, ethanol and water (25mL each; ΔT = 0.14°C/mL). It was deducted that the emerging heat of mixing originates from the difference of endothermic bond breaking and exothermic bond formation which results in an overall heat release. DMF and DMSO are aprotic water-soluble liquids, being neither hydrogen bond donors but acceptors. By replacing the ethanol from the previous experiment with DMF (25mL each; ΔT = 0.32°C/mL) or DMSO (25mL each; ΔT = 0.46°C/mL), the resulting heat is higher, since energy consuming bond breaking between the aprotic solvents is not necessary, while energy releasing bond formation with water as donor molecules occurs. In analogy, we obtained comparable results in our measurements when mixing H_2O/FA, DMF/FA, and DMSO/FA (Table 2; #1-3). In the second part of the paper, the nature of the hydrogen bonds in the water/FA and DMSO/FA system is extensively discussed.

Additionally, we assessed the enthalpy of mixing for formic acid/amine mixtures and FA/KOH, as a representative of an inorganic base (Table 2). The amines were chosen either because they are readily used in CO_2 hydrogenation/hydrogen evolution from FA or because of interesting chemical properties. All measurements were executed in triplicate if not indicated otherwise and we performed ^{1}H-NMR measurements on all our samples before and after mixing to verify the purity of the solvents and to exclude side reactions.

Beginning with the water/FA system (Table 2, #1), the heat of mixing is moderate and peaks at X(water) = 0.71, producing in total 0.76 kJ/mol. In proton NMR spectra, the water and the HCOO**H** NMR signal are seen as one signal since the proton exchange occurs too fast to be resolved on the NMR time scale. The corresponding reaction of DMSO and FA (#2) is approximately 15 times more exothermic and even reaches the level of amine/FA reactions.

Experiments #3 to #7 (Table 2) are dedicated to compounds bearing an amino group and the registered heat releases are in the range of acid-base reactions (KOH/FA, #8). Overall, we observed increasing heat release in the order tertiary > secondary > primary amines. The reactions of primary and secondary amines with formic acid are strongly exothermic and the formation of a colorless solid hindered stirring and caused the interruption of the measurement. Thus it was not possible to ascertain the enthalpy of mixing for cyclohexylamine/FA (pK_a = 10.6). Diisopropylamine/FA resulted in a similarly exothermic reaction as cyclohexylamine/FA, approximately 175 kJ/mol were generated and a colorless solid formed at X(FA) = 0.5. Both #6 and #7 were only tested once since it is evident that the reaction is extremely exothermic and the use of this chemicals in CO_2 hydrogenation reaction solvents leads to the formation of salt-like FA/amine adducts, where the extraction of FA is not trivial. Also with triethylamine (tertiary amine, 40.4 kJ/mol, #5), commonly used as a basic additive,[69] the FA separation is not easily accomplished.[70] The TEA/FA mixture (final X(FA) = 0.5) remained a (viscous) liquid and did not form a slurry or salt. NMR measurements show that both chemicals coexist as distinct peak sets after combing the chemicals (see ESI). DMF interacts with FA more gently and the enthalpy of mixing is with 10.6 kJ/mol comparable to DMSO/FA mixtures.

KOH (1 mole in 54 mL water, #8) is used in experimental procedures to establish basic conditions. Some of the highest TOFs in bicarbonate/carbonate hydrogenation were obtained in KOH basic solutions. The reaction of FA with KOH solution is considerably exothermic (23.6 kJ/mol) and a solvated salt forms.

Entry	Compound A	ΔH_{mix_FA} [kJ/mol]
#1	Water	0.76 ± 0.16
#2	Dimethylsulfoxid (DMSO)	11.6± 0.2
#3	Dimethylformamide (DMF)	10.6 ± 0.9
#4	N,N-Dimethylethylamine	18.1 ± 2.2
#5	Triethylamine (TEA)	40.4 ± 0.9
#6	Diisopropylamine*	175
#7	Cyclohexylamine*	-
#8	KOH (1 mol in water)	24.6 ± 0.7

Table 2 Molar heat of mixing from formic acid and water, DMSO, or an amine; each result is the mean value of three separate measurements with its corresponding standard deviation
**heavily exothermic reaction behavior and formation of a white sold before reaching 1:1 stoichiometry (amine/FA)*

Calorimetric assessment of selected organic solvents/formic acid systems

Over the years, formic acid-based hydrogen storage and delivery was carried out in many organic solvent systems. We measured the enthalpy of mixing for relevant solvents/FA mixtures. These data serve to develop new and optimize old systems. The experimental procedures are analogous to the previously discussed water/FA and DMSO/FA measurements.

Entry	Compound	ΔH_{mix_FA} [kJ/mol]
#1	Methanol (MeOH)*	4.12 ± 0.09
#2	Ethanol (EtOH)*	3.05 ± 0.04
#3	Isopropanol*	1.04 ± 0.03
#4	1,2-Propanediol*	2.34 ± 0.08
#5	2-(Diethylamino)ethanol	21.2 ± 1.6
#6	Tetrahydrofuran	5.40 ± 0.12
#7	Acetone	3.09 ± 0.10
#8	Ethyl acetate	0.93 ± 0.05
#9	Acetophenone	0.49 ± 0.03
#10	Toluene	-0.13 ± 0.06
#11	Dimethyl carbonate (DMC)	-0.22 ± 0.06
#12	Acetonitrile (ACN)	-0.26 ± 0.03
#13	Chloroform	-0.45 ± 0.07
#14	Dichloromethane (DCM)	-0.72 ± 0.02
#15	Nitrobenzene	-0.82 ± 0.06
#16	Nitromethane	-1.51 ± 0.07

Table 3 Molar heat of mixing from formic acid and selected solvents;
**[1]H NMR confirmed a chemical reaction (ester formation)*

Measurements (Table 3, #1 to #5) determine the heat of mixing of relevant alcohols mixed with FA. ^{1}H-NMR spectra recorded 10h after mixing the solvents, confirmed the presence of esters e.g. methyl formate (MeOH/FA) or ethyl formate (EtOH/FA). As mentioned previously, heat flow calorimetry is a quantitative method, so the detected heat flow at the reactor walls is the sum of all ongoing processes in the reactor chamber. Therefore, it cannot be distinguished between the enthalpies of chemical reactions and mixing enthalpies.

Methanol (Table 3, #1) reacts most exothermically of all tested alcohols by releasing 4.12 kJ/mol. The heat evolution is above the average of all tested solvents e.g. ethanol (#2) and isopropanol (#3) show weaker interactions (3.05 kJ/mol and 1.04 kJ/mol, respectively). The emerging heat of 1,2-propanediol/FA is slightly higher (2.34 kJ/mol, #4) than from isopropanol. In 2(diethylamino)ethanol (#5), the alcohol moiety seems to have a neglectable effect on the reaction behavior of the overall heat release of 21.2 kJ/mol and the substance resembles more an amine e.g. Table 3, #5.

In experiment #6, we studied THF/FA mixtures and determined ΔH_{mix} to be 5.40 kJ/mol. The intermediate heat release is an indication for extended interactions between THF and FA, which is in agreement with the circumstance that THF forms acid-base adducts with weak acids,[71] while strong acids cleave the ether. The letter phenomenon was excluded by ^{1}H-NMR measurements as well as the formation of new products in THF/FA mixtures could not be observed (see ESI). Acetone (#7) exhibits a pronounced permanent dipole moment (μ = 2.93 D),[72] which can interact positively with dipolar formic acid (μ = 1.41 D),[73] resulting in a heat release of 3.09 kJ/mol, ^{1}H-NMR . Ethyl acetate (#8) and acetophenone (#9) show similar mixing enthalpies to water and formic acid. For acetophenone, this is probably due to its ketone function which is miscible with FA and exhibits a positive enthalpy of mixing, which is in conversely negative for toluene (-0.13 kJ/mol, #10). Dimethyl carbonate (-0.22 kJ/mol, #11) is often considered as a "green" solvent,[74] but without additives, there are no favorable interactions between formic acid and DMC. The interactions between acetonitrile (ACN, #12) and FA are also slightly endothermic (-0.26 kJ/mol), indicating that the pure compounds are energetically preferred over mixtures. Halogenated solvents, such as chloroform or DCM (#13 and #14) and solvents bearing a nitro function (#15 and #16) seem equally unfitting solvents for CO_2 hydrogenation reactions, since they all show endothermic mixing behavior and reduced miscibility with formic acid.

Considerations about the structures of water/FA and DMSO/FA assemblies based on ATR and NMR spectroscopy

For a more profound analysis of the intermolecular interactions in the water/FA- and the DMSO/FA system, eleven samples of varying concentration were prepared. Subsequently, we analyzed the concentration dependency of the chemical shifts from ^{1}H and ^{13}C nuclei, namely the **H**COOH proton of FA (δ_{CH}), HCOO**H** proton (δ_{OH}), and carbon chemical shifts (H**C**OOH) of formic acid (δ_{COO}), in the water/FA and DMSO/FA system. The chemical shifts were plotted against the mole fraction of formic acid, *X(FA)*. Figure 6 shows the proton shifts and Figure 7 describes the carbon-13 chemical shifts. The monotonic dependencies of the acidic proton (HCOO**H**) differ in all cases significantly from dilution shift curves of the V-type with clear minima at medium concentrations, which we assessed for the DMSO/acetic acid system (Figure 8). These V-type curves were also reported earlier for similar systems, e.g. CH_3COOH mixtures with DMSO[75] or water.[76]

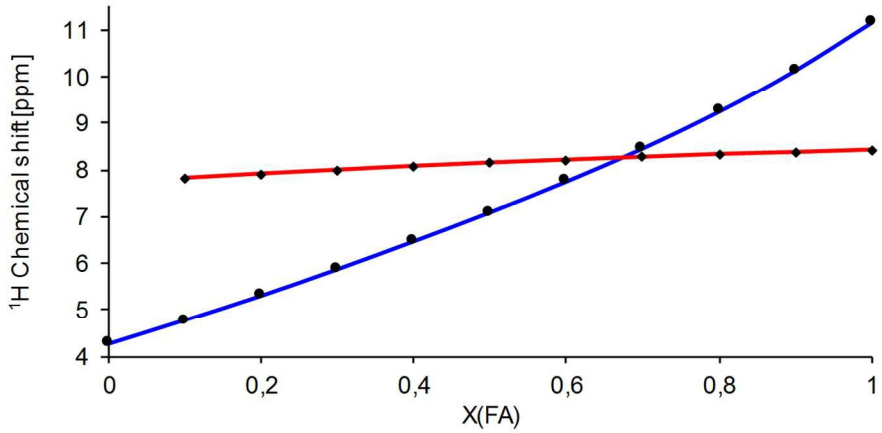

*Figure 6 Dilution shift curves for the water/FA system: chemical shifts of HCOO**H** proton (δ_{OH}, blue, ●) and **H**COOH proton (δ_{CH}, red, ■).*

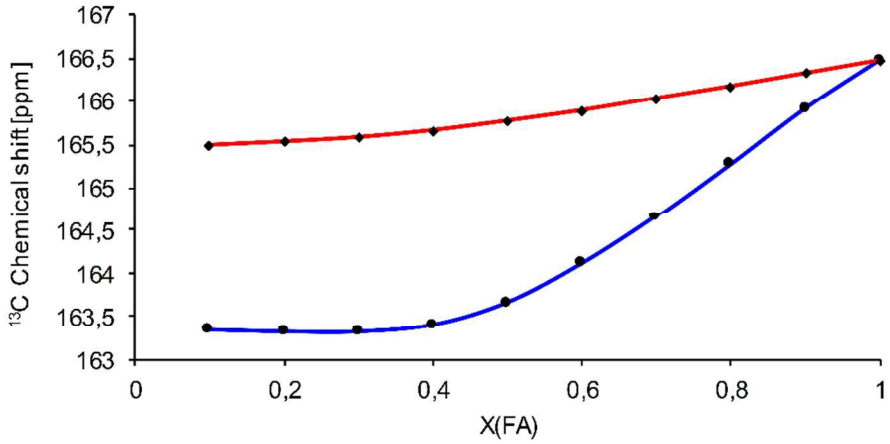

*Figure 7 ^{13}C-NMR chemical shifts δ_{COO}: dilution shift curves for the water/H**C**OOH (red, ■) and DMSO/H**C**OOH (blue, ●) system.*

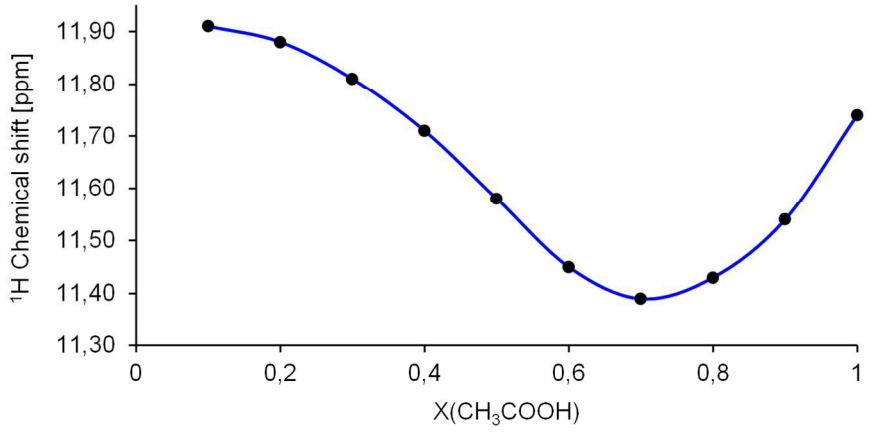

*Figure 8 Typical V-shaped curve for the DMSO/CH_3COO**H** system*

In case of DMSO/CH_3COOH systems, the *V*-type pattern of 'δ_{OH} vs. *X*' plots was assigned to the equilibrium of two aggregates in the solutions - 2(CH_3COOH):1(DMSO) and 1(CH_3COOH):1(DMSO).[75] To determine the number and composition of aggregates formed in the DMSO/FA system, we applied a method[77] based on concentration relationships for the δ_{COO}, δ_{CH} and δ_{OH} chemical shifts. Bogachev *et al.* shows that if only two types of particles (aggregates) coexist in equilibrium with each other in a certain concentration range, then the chemical shifts of the nuclei contained in these species are related to each other by a linear relationship (see ESI).[78, 79] A graph, showing the chemical shifts of δ_{COO} and δ_{CH} (Figure 9), is linear in the range from 1 to 0.5, which indicates that only two types of species containing FA molecules are formed in the solution. Obviously, one type of these species is self-associated FA, and the other is an aggregate of FA and DMSO. At lower concentrations, the chemical shifts remain constant (Figure 7, Figure 9), since the composition of the DMSO-FA adducts do not change (taking the limited precision of an experimental procedure into account). Thus, the stoichiometry of the aggregate is 1:1, and at $X < 0.5$, self-associated FA molecules are no longer present in the solution. Instead, free DMSO molecules appear (not bound to FA molecules). The same stoichiometry of DMSO-FA adducts was confirmed by plotting the chemical shits of δ_{COO} or δ_{CH} versus $(1-X)/X$ (calculations in ESI).

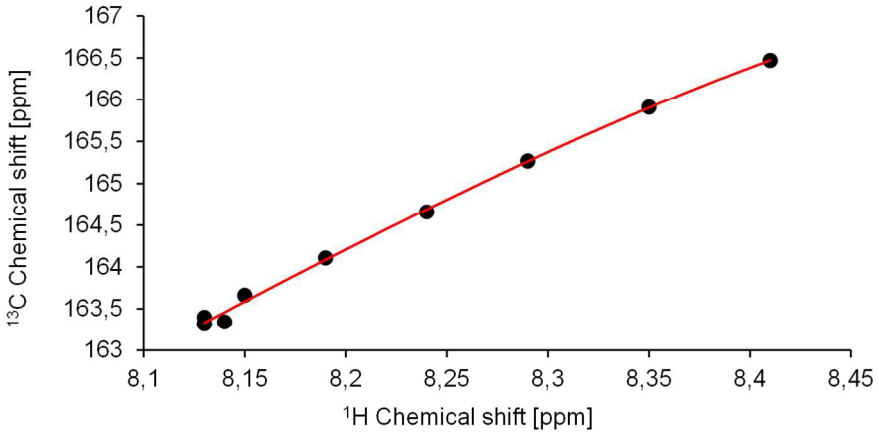

Figure 9 Diagram of δ_{COO} - δ_{CH} chemical shifts for the DMSO/FA system; X(FA) is increasing from left to right; the linear range of the graph indicates that there are only two different species of FA aggregates in solution

For aqueous acetic acid solutions, the *V*-type pattern of 'δ_{COO} vs. *X*' plot (*vide supra*) was assigned to the dissociation of acid at concentrations lower than approx. 40%.[76] The qualitatively different character of the dilution curve shown in Figure 7 suggests that FA in aqueous solutions exists in molecular form (non-dissociated). Our findings are confirmed by earlier published results, based on IR spectra analysis.[40] A mutual dependence of δ_{COO} and δ_{OH} (Figure 10) can be divided into three approximately linear regions corresponding to certain concentration ranges: (i) $0.017 < X <$~0.3; (ii) ~$0.3 < X <$ ~0.75; (iii) ~$0.75 < X < 1$. As mentioned earlier, this suggests that in each region are only two species with FA molecules in their structure. In the region (iii) one of the particles is self-associated FA, while the other is an aggregate with a 1(H_2O)-3(FA) stoichiometry; 2(H_2O)-1(FA) aggregate coexists with "free" water in the region (iii); 1(H_2O)-3(FA) and 2(H_2O)-1(FA) aggregates are in equilibrium in region (ii). This scenario is in conflict with Raman spectroscopic evidence[42] of the presence of the self-associated FA in the concentration range $0.51 \leq X \leq 1$, i.e. these self-associates coexist with 1(H_2O)-3(FA) and 2(H_2O)-1(FA) aggregates at least in the part of the range (ii). The third component is, most probably, present also in region (iii), otherwise

δ_{CH} would not change at X < ~0.3 (Figure 6). There are two possible explanations for the above contradictions: either concentrations of the "extra" species are small, or their chemical shifts do not differ much from the chemical shifts of at least one of the two "main" components in the corresponding concentration ranges.

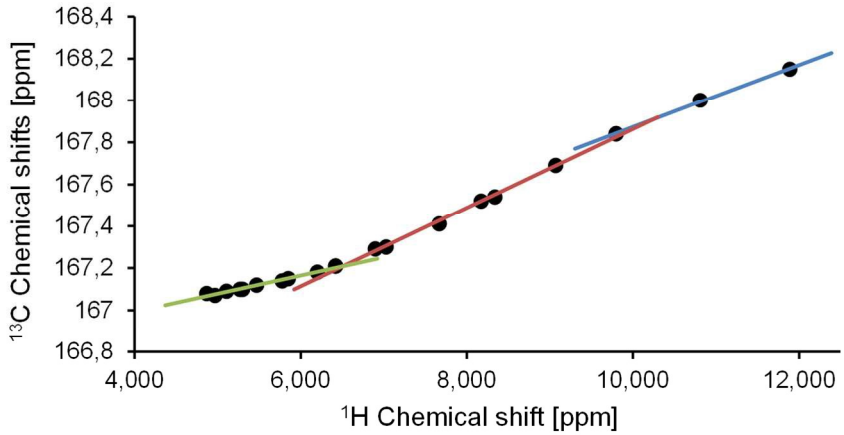

Figure 10 Diagram of δ_{COO} - δ_{OH} chemical shifts for the water/FA system; the three linear regions correspond to certain concentration ranges; in each region are only two species with FA molecules in their structure

To get more information about solute-solvent interactions in aqueous solutions of FA, we performed ATR spectroscopy (attenuated total reflection spectroscopy) of these systems. Distinctive frequencies of clearly assignable and isolated IR bands (stretching vibrations) of C=O and C-H moieties of FA (νC=O and νC-H, respectively) are presented in Table 4. As can be seen, the νC-H band monotonically red-shifts upon dilution of FA solutions until X = 0.2, while νC=O frequencies remains almost constant. In Raman spectra of pure FA,[42] strong self-association effects cause a splitting of the νC=O band into two species at 1725 and 1661 cm^{-1}. This splitting is caused by coupled vibrations of the associated molecules. Dilution of FA with water weakens the association and this results in a decreased peak splitting in the spectrum, which becomes apparent for the most dilute water/FA mixture (X = 0.51) with 1726/1702 cm^{-1}.[42] As shown recently by neutron diffraction method,[80] self-associated species of FA are also present in ca. 35 mol% solution. In the present experiments, the self-association appears to disrupt almost completely at X(0.2) and X(0.1) and the self-associated forms of FA are replaced by aggregates of FA with water of more or less stable composition. This is suggested by the absence of changes of the νC-H band position for these two solutions (Table 4). The carbonyl band for the solutions is quite close to the value reported for 1:2 cluster of FA and water isolated in Ar matrix (Table 4),[39] which suggests that the dominating form of water-FA association in the diluted solutions is the 1:2 aggregate. It should be noted that an *ab initio* molecular dynamics study[52] on the solvation of FA in water also demonstrated a presence of two water molecules in the first coordination shell of FA at room temperature.

	νC-H (IR)	**νC=O (IR)**
Gaseous FA[81]	2943	1770
FA monomer in Ar matrix[39]		1767
FA acyclic dimer in Ar matrix[39]		1747
FA cyclic dimer in Ar matrix[39]		1728
FA-water 1:1 cluster in Ar matrix[39]		1737

FA-water 1:2 cluster in Ar matrix[39]		1722
Liquid (98%) FA	2953	1719
X(FA) = 0.8	2950	1721
X(FA) = 0.5	2947	1717
X(FA) = 0.2	2941	1717
X(FA) = 0.1	2941	1717

Table 4 Frequencies (cm^{-1}) of IR bands of stretching vibrations of C=O and C-H groups of neat formic acid (FA) and FA in aqueous solutions of various concentrations.

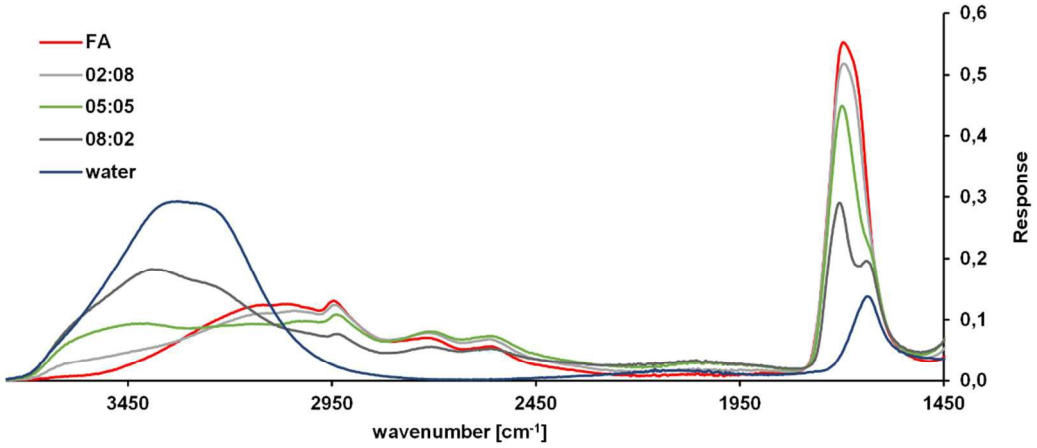

Figure 11 νO-H bands in IR spectrum of pure FA, pure water, and aqueous solutions with mole fractions X(FA) = 0.2, 0.5, and 0.8 (full spectrum in ESI).

A broad and strong νO-H band for self-associated FA at ca. 3150 cm^{-1} can be clearly seen in the ATR spectra of aqueous solutions with mole fractions *X*(FA) = 0.8 and 0.5 (Figure 11), which suggests a presence of essential amounts of self-associated FA in these solutions. Thus, dominating forms of hydrated FA at *X*(FA) = 0.5 could not be 1(H_2O)-3(FA), 1(H_2O)-2(FA) or 1(H_2O)-1(FA), and the conclusion of the preceding paragraph about formation of 2(H_2O)-1(FA) aggregate is in agreement with the spectra shown in Figure 11. When the broad νOH band of self-associated FA vanishes, a broad absorption in the region ~3600 - 1800 cm^{-1} appears, which is less intense than in the case with DMSO solutions (Figure 12). This absorbance is caused by the water-FA hydrogen bonds (H-bonds). The bands observed in the region ~2900-2400 cm^{-1} are caused by overtones and combination vibrations intensified by Fermi resonance with the fundamental transition.[82] The "center of gravity" of the absorbance in the region ~3400 - 1800 cm^{-1} caused by DMSO-FA H-bonds (Figure 12) is red-shifted relative to the case of aqueous solutions. The red shift and the intensification of this broad feature means stronger DMSO-FA H-bonding relative to water/FA system.

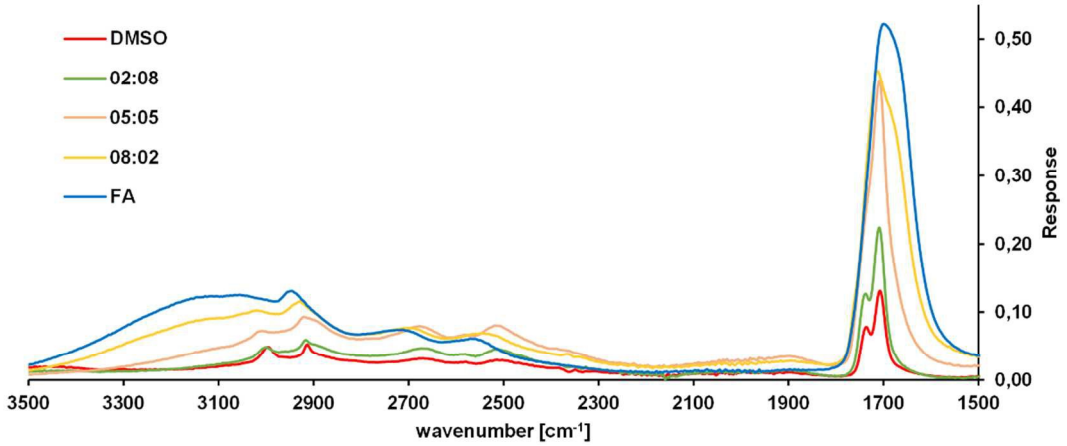

Figure 12 IR spectrum of pure FA, DMSO and mixtures with mole fractions X(FA) = 0.2, 0.5, and 0.8 (full spectrum in ESI).

Structures of DMSO-FA and $2H_2O$-FA aggregates deduced on the basis of NMR and IR spectroscopic data were optimized in silico (Figure 13, see Materials and Methods) and corresponded to minima on potential energy surface. According to the computations H-bonds between FA and DMSO are stronger than H-bonds formed with water molecules: i) the H…O bond is shorter and ii) frequency of stretching vibrations νO-H is lower in the DMSO-FA aggregate than in $2H_2O$-FA aggregate; iii) the computed IR intensity of νO-H (1778 km/mol) in DMSO-FA aggregate is higher than 1387 km/mol, calculated for νO-H in the $2H_2O$-FA aggregate. Thus, quantum chemical computations corroborate conclusions made on the basis of spectroscopic experiments.

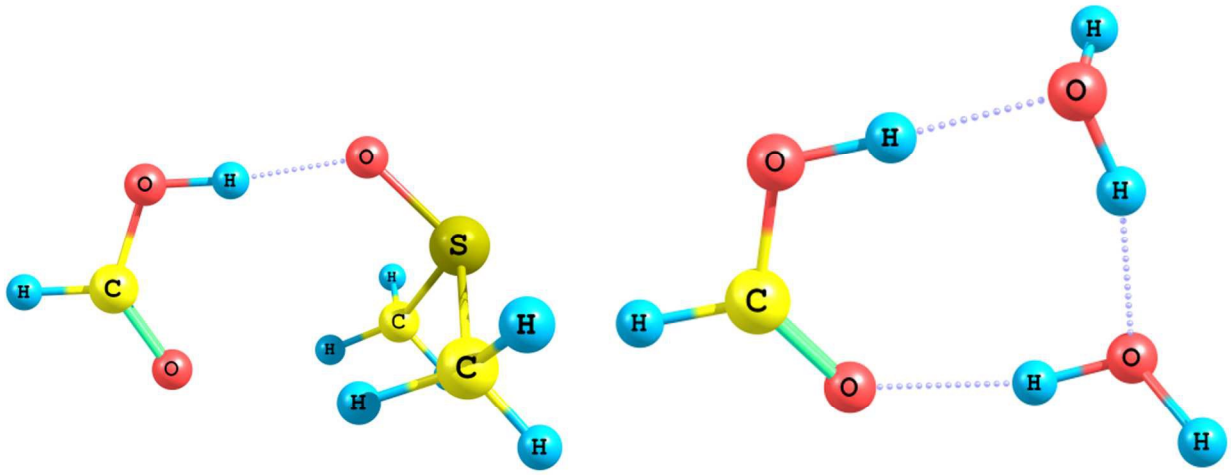

Figure 13 B3PW91/aug-cc-pVTZ optimized structures of DMSO-FA (left) and $2H_2O$-FA (right) aggregates. The main characteristics of hydrogen bonds shown with dotted lines are the following: DMSO-FA, d(H…O) = 1.61 Å; vO-H = 2955 cm^{-1}; $2H_2O$-FA, d(H…O) = 1.62 Å; vO-H = 2965 cm^{-1}

In conclusion, we quantified the enthalpy of mixing for water and several organic solvents with formic acid by heat flow calorimetry. The heat of mixing for water and FA showed a distinctly different behavior by reacting most exothermically at a certain mole fraction (X(water) = 0.7) and not when the pure chemicals were combined as was observed for the other scrutinized solvents (Figure 4). The results from our calorimetric examinations are valuable contributions for developing large scale hydrogen

storage applications and for formic acid as a portable/mobile hydrogen source by estimating the energy, which is necessary to liberate hydrogen under these circumstances. The DMSO/FA and water/FA systems were further examined with spectroscopic methods (multinuclear NMR and ATR) and allowed us to identify the different adducts in both systems, whose prevalence depends on the concentration. These data were further corroborated with quantum chemical calculations and finally used to draw mutual DMSO-FA and water-FA structures, revealing stronger hydrogen bonds in the DMSO/FA system.

Material and Methods

Materials

All chemicals were used as obtained from Sigma Aldrich (DMSO, analytical grade) or Merck (formic acid, 98-100% purity). All solvents had at least HPLC grade and were used without further purification. Water was deionized (Milli-Q Integral 5), meeting the ISO 3696 (1987), Grade 3 water standard in terms of conductivity (G = 2.347 µS/cm). Glassware (vessels), which was used the experiments, was cleaned in a base bath, acid bath, subsequently rinsed with deionized water, then acetone, and finally dried at 190°C.

Instruments

The calorimetric measurements were accomplished with a Mettler Toledo EasyMax 102 Advanced Synthesis Workstation with HFCal option (heat flow calorimetry) at atmospheric pressure. The reaction chamber's temperature was set to 25.0°C. Data treatment was done with iControl 5.2.219 SP1 software. The IR spectra were recorded with an attenuated total reflection spectrometer (Varian FTS 800 FT-IR, Scimitar Series). Conductometry data was acquired on a Metrohm 712 Conductometer equipped with a Pt1000 measuring probe at 25°C. NMR spectra were collected with a Bruker AV-400 (5 mm) and AVIII-400. MestReNova 10.0.1 was used for spectra evaluation.

Methods

Calorimetric measurement

In general, one compound (formic acid or a solvent) was prefilled into the reactor (first fill) and allowed to reach thermal equilibrium, then the heat capacity of the substance was assessed. Subsequently, the second compound was added incrementally while the machine was programmed to keep the temperature in the reactor chamber constant (active heating or cooling through reactor walls). The next portion only added when thermal equilibrium was reached. The integrals over time of the heat flow through the reactor walls were used to determine the enthalpies of mixing.

Some measurements required more sophisticated experimental techniques like splitting one experiment in two discrete parts because of the limited volumetric capacity of the measuring chamber (relevant for Figure 2 and Figure 4). In both cases, the first additions were done in one experiment, the remaining ones in a second. In practice, 55 mL of the produced water/FA or DMSO/FA mixture was kept for continuing the experiment in a second part. The injected FA volumes in the second experiment were adapted to the altered starting conditions to correspond to 0.25 mole from the first experiment (Figure 2, addition 7-21; Figure 4, addition 5-17).

Computations

All quantum chemical calculations were carried out using the Gaussian 03 suite of programs.[83] Following full geometry optimizations, harmonic vibrational frequencies and infrared intensities were calculated by density functional theory (DFT) method employed in this study, corresponding to the Becke`s three-parameter exchange functional[84] in combination with the Perdew and Wang 1991 gradient-corrected correlation functional (B3PW91).[85] The "correlation consistent" aug-cc-pVTZ basis set was used.[86]

Acknowledgement

The Swiss Competence Center for Energy Research (SCCER), Commission for Technology and Innovation (CTI), and EPFL are thanked for financial support. We also thank Mettler-Toledo for supporting our research.

References

1. D. Mori and K. Hirose, *Int. J. Hydrogen Energy*, 2009, **34**, 4569-4574.
2. M. Balat, *Int. J. Hydrogen Energy*, 2008, **33**, 4013-4029.
3. World Resources Institute, CAIT Climate Data Explorer, World Resources Institute, http://cait.wri.org, (accessed 14/10, 2015).
4. O. G. J. Jos, J.-M. Greet, M. Marilena and P. A. H. W. Jeroen, *Trends in global CO2 emissions: 2014 report*, The Hague, 2014.
5. Intergovernmental Panel on Climate Change (IPCC), *Climate Change 2007: Synthesis Report. Contribution of Working Groups I, II and III to the Fourth Assessment Report of the Intergovernmental Panel on Climate Change*, Intergovernmental Panel on Climate Change (IPCC), Geneva, Switzerland, 2007.
6. M. E. Boot-Handford, J. C. Abanades, E. J. Anthony, M. J. Blunt, S. Brandani, N. Mac Dowell, J. R. Fernandez, M.-C. Ferrari, R. Gross, J. P. Hallett, R. S. Haszeldine, P. Heptonstall, A. Lyngfelt, Z. Makuch, E. Mangano, R. T. J. Porter, M. Pourkashanian, G. T. Rochelle, N. Shah, J. G. Yao and P. S. Fennell, *Energy Environ. Sci.*, 2014, **7**, 130-189.
7. Z. Zhang, S. Hu, J. Song, W. Li, G. Yang and B. Han, *ChemSusChem*, 2009, **2**, 234-238.
8. K. V. Raghavan and B. M. Reddy, *Industrial Catalysis and Separations: Innovations for Process Intensification*, Apple Academic Press, 2014.
9. Intergovernmental Panel on Climate Change. Working Group III., *Carbon Dioxide Capture and Storage: Special Report of the Intergovernmental Panel on Climate Change*, Cambridge University Press, 2005.
10. D. A. Bryant and N.-U. Frigaard, *Trends Microbiol.*, 2006, **14**, 488-496.
11. G. Marbán and T. Valdés-Solís, *Int. J. Hydrogen Energy*, 2007, **32**, 1625-1637.
12. S. Sharma and S. K. Ghoshal, *Renew. Sust. Energ. Rev.*, 2015, **43**, 1151-1158.
13. P. P. Edwards, V. L. Kuznetsov, W. I. F. David and N. P. Brandon, *Energy Policy*, 2008, **36**, 4356-4362.
14. M. Grasemann and G. Laurenczy, *Energy Environ. Sci.*, 2012, **5**, 8171-8181.
15. A. F. Dalebrook, W. Gan, M. Grasemann, S. Moret and G. Laurenczy, *Chem. Commun.*, 2013, **49**, 8735-8751.
16. P. G. Jessop, T. Ikariya and R. Noyori, *Nature*, 1994, **368**, 231-233.
17. S. Wesselbaum, U. Hintermair and W. Leitner, *Angew. Chem. Int. Ed.*, 2012, **51**, 8585-8588.
18. C. Federsel, R. Jackstell and M. Beller, *Angew. Chem.*, 2010, **122**, 6392-6395.
19. P. G. Jessop, T. Ikariya and R. Noyori, *Chem. Rev.*, 1995, **95**, 259-272.
20. W. Leitner, *Angew. Chem. Int. Ed.*, 1995, **34**, 2207-2221.
21. M. Aresta, A. Dibenedetto and E. Quaranta, *Reaction Mechanisms in Carbon Dioxide Conversion*, Springer Berlin Heidelberg, 2015.
22. X. Li, X. Ma, F. Shi and Y. Deng, *ChemSusChem*, 2010, **3**, 71-74.
23. D. Preti, S. Squarcialupi and G. Fachinetti, *Angew. Chem.*, 2010, **122**, 2635-2638.
24. P. G. Jessop, F. Joó and C.-C. Tai, *Coord. Chem. Rev.*, 2004, **248**, 2425-2442.
25. C. Federsel, R. Jackstell and M. Beller, *Angew. Chem. Int. Ed.*, 2010, **49**, 6254-6257.
26. C. A. Huff and M. S. Sanford, *ACS Catalysis*, 2013, **3**, 2412-2416.
27. B. Loges, A. Boddien, H. Junge and M. Beller, *Angew. Chem. Int. Ed.*, 2008, **47**, 3962-3965.
28. S. Moret, P. J. Dyson and G. Laurenczy, *Nat. Commun.*, 2014, **5**.
29. A. Boddien, F. Gärtner, R. Jackstell, H. Junge, A. Spannenberg, W. Baumann, R. Ludwig and M. Beller, *Angew. Chem. Int. Ed.*, 2010, **49**, 8993-8996.
30. A. Boddien, B. Loges, F. Gärtner, C. Torborg, K. Fumino, H. Junge, R. Ludwig and M. Beller, *J. Am. Chem. Soc.*, 2010, **132**, 8924-8934.

31. A. Boddien, B. Loges, H. Junge and M. Beller, *ChemSusChem*, 2008, **1**, 751-758.
32. C. Fellay, P. J. Dyson and G. Laurenczy, *Angew. Chem. Int. Ed.*, 2008, **47**, 3966-3968.
33. S. Oldenhof, B. de Bruin, M. Lutz, M. A. Siegler, F. W. Patureau, J. I. van der Vlugt and J. N. H. Reek, *Chem. Eur. J*, 2013, **19**, 11507-11511.
34. Y. Manaka, W.-H. Wang, Y. Suna, H. Kambayashi, J. T. Muckerman, E. Fujita and Y. Himeda, *Catal. Sci. Tech.*, 2014, **4**, 34-37.
35. F. M. Kerton and R. Marriott, *Alternative Solvents for Green Chemistry*, Royal Society of Chemistry, 2013.
36. G. Wypych, *Handbook of Solvents*, ChemTec, 2001.
37. D. Priem, T.-K. Ha and A. Bauder, *J. Chem. Phys.*, 2000, **113**, 169-175.
38. K. Marushkevich, L. Khriachtchev and M. Räsänen, *J. Phys. Chem. A*, 2007, **111**, 2040-2042.
39. L. George and W. Sander, *Spectrochim. Acta Mol. Biomol. Spectrosc.*, 2004, **60**, 3225-3232.
40. M. Leuchs and G. Zundel, *J. Chem. Soc., Faraday Trans.*, 1980, **76**, 14-25.
41. M. Śmiechowski, E. Gojło and J. Stangret, *J. Phys. Chem. B*, 2011, **115**, 4834-4842.
42. R. J. Bartholomew and D. E. Irish, *J. Raman Spectrosc.*, 1999, **30**, 325-334.
43. P. Waldstein and L. A. Blatz, *J. Phys. Chem.*, 1967, **71**, 2271-2276.
44. S. Aloisio, P. E. Hintze and V. Vaida, *J. Phys. Chem. A*, 2001, **106**, 363-370.
45. Z. Zhou, Y. Shi and X. Zhou, *J. Phys. Chem. A*, 2004, **108**, 813-822.
46. D. K. Maity, *J. Phys. Chem. A*, 2013, **117**, 8660-8670.
47. D. Wei, J.-F. Truchon, S. Sirois and D. Salahub, *J. Chem. Phys.*, 2002, **116**, 6028-6038.
48. K. Chuchev and J. J. BelBruno, *J. Mol. Struct.*, 2006, **763**, 199-204.
49. A. Galano, M. Narciso-Lopez and M. Francisco-Marquez, *J. Phys. Chem. A*, 2010, **114**, 5796-5809.
50. R. M. Aminova, G. A. Schamov and A. V. Aganov, *J. Mol. Struct.*, 2000, **498**, 233-246.
51. J.-G. Lee, E. Asciutto, V. Babin, C. Sagui, T. Darden and C. Roland, *J. Phys. Chem. B*, 2006, **110**, 2325-2331.
52. L. Z. Chen Qiubo, Wong Chee How, *J. Chem. Theory Comput.*, 2012, **11**, 1019-1032.
53. R. Iftimie, D. Salahub, D. Wei and J. Schofield, *J. Chem. Phys.*, 2000, **113**, 4852-4862.
54. H. Piekarski, *Thermochim. Acta*, 2004, **420**, 13-18.
55. J. H. Seinfeld and S. N. Pandis, *Atmospheric Chemistry and Physics: From Air Pollution to Climate Change*, Wiley, 2012.
56. Q. Appleton, L. Bernander and G. Olofsson, *Tetrahedron*, 1971, **27**, 5921-5931.
57. G. Gatti, A. Levi, V. Lucchini, G. Modena and G. Scorrano, *J. Chem. Soc., Chem. Commun.*, 1973, 251-252.
58. G. A. Olah, A. T. Ku and J. A. Olah, *J. Org. Chem.*, 1970, **35**, 3904-3908.
59. G. A. Olah, A. M. White and D. H. O'Brien, *Chem. Rev.*, 1970, **70**, 561-591.
60. M. Spiekermann and B. Schrader, *Angew. Chem. Int. Ed.*, 1977, **16**, 197-198.
61. F. Tureček, *J. Phys. Chem. A*, 1998, **102**, 4703-4713.
62. G. A. Olah and D. A. Klumpp, *Superelectrophiles and Their Chemistry*, Wiley, 2008.
63. J. Barrett, *Inorganic Chemistry in Aqueous Solution*, Royal Society of Chemistry, 2003.
64. E. Buncel, M. Decouzon, A. Formento, J.-F. Gal, M. Herreros, L. Li, P.-C. Maria, I. Koppel and R. Kurg, *J. Am. Soc. Mass. Spectrom.*, 1997, **8**, 262-269.
65. S. G. Lias, J. F. Liebman and R. D. Levin, *Evaluated gas phase basicities and proton affinities of molecules, heats of formation of protonated molecules*, American Chemical Society and the American Institute of Physics for the National Bureau of Standards, New York; Washington, D.C., 1984.
66. W. Boyes, *Instrumentation Reference Book*, Elsevier Science, 2009.
67. J. P. Guthrie, *Can. J. Chem.*, 1978, **56**, 2342-2354.
68. N. Friedman, *J. Chem. Educ.*, 1977, **54**, 248.

69. D. Preti, C. Resta, S. Squarcialupi and G. Fachinetti, *Angew. Chem. Int. Ed.*, 2011, **50**, 12551-12554.
70. T. Schaub and R. A. Paciello, *Angew. Chem. Int. Ed.*, 2011, **50**, 7278-7282.
71. C. H. Yoder, P. A. Leber and M. W. Thomsen, *The Bridge To Organic Chemistry: Concepts and Nomenclature*, Wiley, 2010.
72. Z. K. O. Dorosh, *Acta Phys. Pol., A*, 2007, **112**, 95-104.
73. H. Kim, R. Keller and W. D. Gwinn, *J. Chem. Phys.*, 1962, **37**, 2748-2750.
74. C. B. Kreutzberger, *Chloroformates and Carbonates*, John Wiley & Sons, Inc., 2000.
75. H. Fujiwara, *J. Phys. Chem.*, 1974, **78**, 1662-1666.
76. V. G. Khutsishvili, Y. S. Bogachev, M. Y. Belov, S. N. Novikov and N. N. Shapet'ko, *Zh. Obshch. Khim.*, 1986, **56**, 1895-1902.
77. N. N. S. k. Yu. S. Bogachev, *Zh. Obshch. Khim.*, 1988, **62**, 2617-2631.
78. V. G. Khutsishvili, Y. S. Bogachev and N. N. Shapet'ko, *Theor. Exp. Chem.*, 1991, **27**, 72-79.
79. V. G. Khutsishvili, Y. S. Bogachev and N. N. Shapet'ko, *Zh. Phys. Khim.*, 1988, **62**, 2617-2631.
80. S. Soffientini, L. Bernasconi and S. Imberti, *J. Mol. Liq.*, 2015, **205**, 85-92.
81. Y. Maréchal, *J. Chem. Phys.*, 1987, **87**, 6344-6353.
82. H. Wolff, B. Nikolaus and E. Wolff, *J. Chem. Phys.*, 1976, **65**, 3394-3396.
83. *Gaussian 03 (Revision D.02)*. Gaussian, Inc., 2004.
84. A. D. Becke, *J. Chem. Phys.*, 1993, **98**, 5648-5652.
85. J. P. Perdew and Y. Wang, *Physical Review B*, 1992, **45**, 13244-13249.
86. D. E. Woon and T. H. Dunning, *J. Chem. Phys.*, 1993, **99**, 3730-3737.

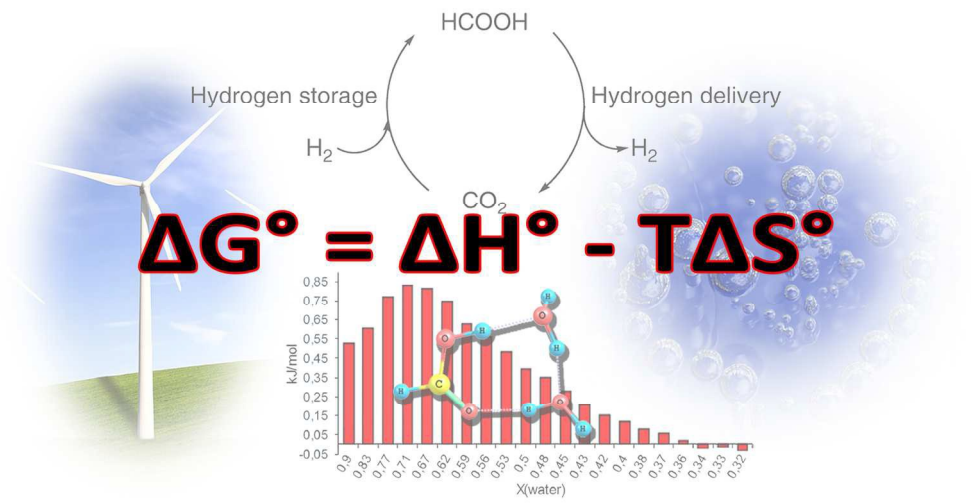

666x333mm (72 x 72 DPI)

Graphical abstract text:

Role of the solvent interactions in H_2-storage/delivery in the carbon dioxide-formic acid couple.